Unmanned Systems, Vol. 14, No. 3 (2026) 657–667

DOI: 10.1142/S2301385026410049

UNMANNED SYSTEMS
https://www.worldscientific.com/worldscinet/us

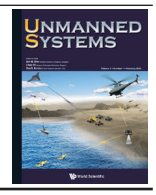

Output-Feedback Optimal Control to Prevent Hypotension Associated with Labor Epidural Anesthesia

Zijian Yang*, Yuchen Dong*, Weinan Gao*,‡,¶, Quan Na†,§,¶, Tengfei Liu*

*State Key Laboratory of Synthetical Automation for Process Industries, Northeastern University, Shenyang 110819, P. R. China

†Department of Obstetrics and Gynecology, Shengjing Hospital of China Medical University, Shenyang 110004, P. R. China

In obstetric anesthesia, maintaining the stability of maternal hemodynamic systems is crucial for the safety of both maternal and fetal well-beings. To achieve this goal, manual infusion method is usually used that infuses phenylephrine to patients during surgery. However, traditional manual infusion method may lead to insufficient precision in the dosage. Although automatic control techniques may improve the accuracy of infusion, the implementation of closed-loop pressure control systems usually depends on the full measurement of states, which is hard or impossible to acquire. In this paper, based on auto-regressive with exogenous input models, an output-feedback optimal controller is developed that integrates a state reconstruction technique and an optimal state-feedback control policy. The proposed method effectively compensates for hypotension induced by bupivacaine through precise infusion of phenylephrine. Simulation results demonstrate that the proposed control method can efficiently regulate mean arterial pressure of patients.

Keywords: Labor epidural anesthesia; mean arterial pressure regulation; hypotension; state reconstruction; optimal output-feedback control.

US

1. Introduction

Anesthesia plays a vital role in childbirth, with epidural anesthesia being frequently employed to effectively relieve the pain while ensuring maternal safety [1]. For instance, bupivacaine is the local anesthetic that is most commonly used in epidural anesthesia. However, improper administration of bupivacaine can induce vasodilation mediated by sympathetic blockade, resulting in hemodynamic imbalance [2] and leading to arterial hypotension. Low blood pressure may cause maternal dizziness, nausea, vomiting, and can further result in fetal acidosis and hypoxia [3, 4]. Therefore, precise blood pressure regulation during anesthesia, especially to counteract hypotension, remains a critical clinical challenge [5].

Recent research in obstetric anesthesia has provided new insights into the mechanisms of hypotension induced by epidural anesthesia and its clinical significance. Tan *et al*. [6] analyzed the maternal cardiovascular responses to spinal anesthesia and highlighted the importance of maintaining adequate uteroplacental perfusion. Mitra *et al*. [7] further summarized best practices for managing maternal hypotension during cesarean delivery, emphasizing the need for precise and responsive vasopressor administration.

Received 5 November 2025; Accepted 8 December 2025; Published 14 February 2026. This paper was recommended for publication in its revised form by Special Issue Editors, Jie Chen, Ben M Chen, and Zongli Lin.
Email Address: ‡*gaown@mail.neu.edu.cn*, §*naquan@163.com*
¶Corresponding authors.

Ahmed *et al*. [8] compared phenylephrine and norepinephrine as vasopressors and emphasized the clinical importance of maintaining stable, well-regulated arterial pressure during obstetric anesthesia. Therefore, it is clear that maintaining blood pressure during anesthesia is critically important.

To maintain blood pressure stability, phenylephrine (PE), a vasopressor, is frequently infused to counteract the hypotension effects of bupivacaine by inducing vasoconstriction [9]. Traditional blood pressure control methods rely on manual infusion, however, this approach has limitations. For instance, manual infusion often lacks sufficient responsiveness and precision amid rapid physiological changes, pharmacokinetic delays, and inter-patient variability [10]. These limitations can lead to hypertensive overshoots or delayed corrections, both of which pose significant risks to maternal and fetal health. Over-infusion may cause placental vasoconstriction, reduce fetal blood flow, and lead to fetal hypoxia. Moreover, delayed PE infusion may fail to correct hypotension promptly, increasing the risk of maternal organ injury or fetal acidosis. Therefore, accurate and prompt infusion of PE is essential to ensure the safety of both the mother and fetus during anesthesia [11].

Considering the specific challenges of blood pressure regulation in obstetric anesthesia, automatic control technologies provide a promising solution. These technologies have been implemented and proven effective in various engineering fields, ranging from smart manufacturing systems [12, 13] to autonomous vehicles [14, 15].

In clinical settings, automatic regulation has already been applied in different directions such as respiratory-ventilator synchronization [16], blood glucose management through artificial pancreas systems [17–19], and hemodynamic stability maintenance in artificial heart devices [20, 21]. Specifically, in the context of blood pressure regulation, Tan *et al*. [6] proposed a rule-based blood pressure control method. Malagutti *et al*. [22] proposed a model-based robust blood pressure control method. Davoud *et al*. [23] introduced a model-free blood pressure control method based on adaptive dynamic programming. However, both model-based and model-free methods essentially rely on state feedback. For the state-space representation derived from auto-regressive with exogenous inputs (ARX) models, some states may lack clear physical interpretations and cannot be directly measured. Therefore, it is necessary to develop output-feedback control methods that preserve the optimality of the closed-loop system.

In this paper, we present a novel method for blood pressure regulation in obstetric anesthesia. The method integrates optimal control and output-feedback control techniques. To address the challenge of unmeasurable or nonphysiological states, we implement a state reconstruction technique that estimates system states in real-time using available input-output data, thereby enabling optimal output-feedback control [24, 25]. The proposed optimal output-feedback control strategy minimizes blood pressure fluctuations, suppresses overshoot, and avoids excessive drug infusion. Furthermore, the method achieves robust mean arterial pressure (MAP) regulation under partial state unmeasurability while adapting to individual patient responses and unexpected clinical disturbances. Simulation results confirm that this integrated optimal output-feedback control method effectively regulates blood pressures.

The contributions of this paper are listed as follows:

(1) Based on the ARX pharmacodynamic model established in [26], this study derives a state-space representation and designs an optimal feedback-feedforward controller. The feedback control action adjusts infusion rates based on real-time MAP measurements, while the feedforward component regulates mean arterial pressure within a safe range. This dual-loop framework ensures robust maintenance of transient hemodynamic stability in parturients.
(2) By incorporating the state reconstruction technique, this study develops an optimal output-feedback control method that enables the MAP to stay within a narrow range around the desired setpoint, even under partial state unmeasurability. This approach effectively addresses clinical constraints where only MAP can be measured. The stability of the proposed control strategy is rigorously analyzed with comprehensive safety guarantees established for clinical implementation.

The remainder of the paper is organized as follows. Section 2 establishes the pharmacodynamic model through system identification, capturing dynamic drug response relationships with embedded time-delay characteristics to reflect clinical realities. This model is subsequently converted into a state-space representation to facilitate controller design. Section 3 presents the theoretical framework integrating state reconstruction with feedforward-feedback optimal control. This section addresses the unmeasurability of the partial state and formulates the theoretical foundation for the control strategy. The stability analysis for the closed-loop system is shown in Sec. 4, ensuring theoretical guarantees for clinical safety. Section 5 validates the controller's disturbance rejection capability through simulations, demonstrating robust blood pressure regulation under clinically relevant perturbations. Section 6 discusses clinical adaptability and proposes future enhancements through adaptive mechanisms. Section 7 concludes with a translational roadmap bridging theoretical advances to clinical implementation.

Notations. Throughout this paper, $\mathbb{R}$ denotes the set of real numbers and $\mathbb{Z}_+$ denotes the set of nonnegative integers. $\|\cdot\|$

represents the Euclidean norm of vectors and the induced matrix norm of matrices. For a square matrix $A \in \mathbb{R}^{n\times n}$, the trace of A is denoted by $\mathrm{Tr}(A)$. For a symmetric matrix $P \in \mathbb{R}^{n\times n}$, $\lambda_m(P)$ stands for the minimum eigenvalue of P, $P \succ 0$ denotes that P is a positive definite matrix.

2. System Modeling

The ARX is a system identification model that has been employed to model physiological systems effectively, see, e.g. cerebral autoregulation system [27]. For the anesthesia situation detailed in [26], the ARX model is mathematically described as

$$\mathcal{A}(z^{-1})y_k = \mathcal{B}(z^{-1})u_k + \mathcal{C}(z^{-1})d_k, \tag{1}$$

where y_k represents the difference between the MAP of patient and its reference at the step k, u_k represents the infusion of PE, d_k represents the infusion of bupivacaine. $A(z^{-1})$, $B(z^{-1})$, and $C(z^{-1})$ are polynomials in the unit delay operator z^{-1}:

$$\begin{cases} \mathcal{A}(z) = z^{-1} + 0.19z^{-2} + 0.07z^{-3}, \\ \mathcal{B}(z) = 0.009z^{-3}, \\ \mathcal{C}(z) = -1.2z^{-5}. \end{cases} \tag{2}$$

To facilitate the design of an output-feedback controller, the ARX model is reformulated into a state-space representation required for output-feedback controller design, the following state variables are defined

$$\begin{aligned} x_{1k} &= y_k, \\ x_{2k} &= -0.19 \times y_{k-1} + 0.07 \times y_{k-2} \\ &\quad + 0.009 \times u_{k-1} - 1.2 \times d_{k-4}, \\ x_{3k} &= 0.07 \times y_{k-1} + 0.009 \times u_k \\ &\quad - 1.2 \times d_{k-3}, \\ x_{4k} &= -1.2 \times d_{k-2}, \\ x_{5k} &= -1.2 \times d_{k-1}. \end{aligned} \tag{3}$$

Given the lumped state $x_k \in \mathbb{R}^5$, the input $v_k = [u_k\ d_k]^{\mathrm{T}} \in \mathbb{R}^2$, and the output $y_k \in \mathbb{R}$, the difference equation can be transformed into the following state-space representation:

$$\begin{aligned} x_{k+1} &= Ax_k + B_v v_k, \\ y_k &= Cx_k, \end{aligned} \tag{4}$$

where

$$A = \begin{bmatrix} 1 & 1 & 0 & 0 & 0 \\ -0.19 & 0 & 1 & 0 & 0 \\ 0.07 & 0 & 0 & 1 & 0 \\ 0 & 0 & 0 & 0 & 1 \\ 0 & 0 & 0 & 0 & 0 \end{bmatrix} \in \mathbb{R}^{5\times 5},$$

$$B_v = \begin{bmatrix} 0 & 0 \\ 0 & 0 \\ 0.009 & 0 \\ 0 & 0 \\ 0 & -1.2 \end{bmatrix} \in \mathbb{R}^{5\times 2},$$

$$C = \begin{bmatrix} 1 & 0 & 0 & 0 & 0 \end{bmatrix} \in \mathbb{R}^{1\times 5}.$$

3. Optimal Output-Feedback Controller Design

3.1. *State reconstruction*

In the state-space representation (4), only the output y_k in the state vector x_k is directly measurable. To design an output-feedback control with limited measurements, state reconstruction is introduced to estimate the full states, allowing for controller design even when some states cannot be measured directly.

Considering the discrete-time linear system (4), it can be checked that the pair (A, B_v) is controllable and the pair (A, C) is observable.

The state reconstruction equation using input and output sequences on time horizon $[k-5, k-1]$ can be written as

$$\begin{aligned} x_k &= A^5 x_{k-5} + V\bar{v}_{k-1,k-5}, \\ \bar{y}_{k-1,\,k-5} &= U x_{k-5} + T\bar{v}_{k-1,k-5}, \end{aligned} \tag{5}$$

where two vectors are defined as follows:

$$\begin{aligned} \bar{v}_{k-1,k-5} &= [v_{k-1}^{\mathrm{T}}, v_{k-2}^{\mathrm{T}}, v_{k-3}^{\mathrm{T}}, v_{k-4}^{\mathrm{T}}, v_{k-5}^{\mathrm{T}}]^{\mathrm{T}}, \\ \bar{y}_{k-1,k-5} &= [y_{k-1}, y_{k-2}, y_{k-3}, y_{k-4}, y_{k-5}]^{\mathrm{T}}. \end{aligned}$$

Matrices V, U and T are given by

$$V = [B_v, AB_v, \dots, A^4 B_v],$$

$$U = [(CA^4)^{\mathrm{T}}, \dots, (CA)^{\mathrm{T}}, C^{\mathrm{T}}]^{\mathrm{T}},$$

$$T = \begin{bmatrix} 0 & CB_v & CAB_v & CA^2B_v & CA^3B_v \\ 0 & 0 & CB_v & CAB_v & CA^2B_v \\ 0 & 0 & 0 & CB_v & CAB_v \\ 0 & 0 & 0 & 0 & CB_v \\ 0 & 0 & 0 & 0 & 0 \end{bmatrix}.$$

Since the system (4) is observable, there exists a left inverse of U such that $U^+ = [U^{\mathrm{T}}U]^{-1}U^{\mathrm{T}}$. The following

lemma recalled from [28] demonstrates that the system state can be reconstructed using input/output sequences.

Lemma 3.1. *The state of the system* (4), x_k, *can be uniquely obtained from the measured input/output sequences by*

$$x_k = \begin{bmatrix} M_u, M_y \end{bmatrix} \begin{bmatrix} \bar{v}_{k-1,\,k-5} \\ \bar{y}_{k-1,\,k-5} \end{bmatrix} = \Theta z_k, \tag{6}$$

where $M_y = A^N U^+$, $M_u = V - M_y T$, $\Theta = \begin{bmatrix} M_u, M_y \end{bmatrix}$, *and* $z_k = \begin{bmatrix} v_{k-1,\,k-5}^{\mathrm{T}} & y_{k-1,\,k-5}^{\mathrm{T}} \end{bmatrix}^{\mathrm{T}}$.

3.2. *Optimal state-feedback controller*

According to clinical practice guidelines for blood pressure management, the following two control objectives need to be achieved.

(1) Under the influence of physiological variations and drug injections, the MAP stays within a safe range around the setpoint.
(2) The transient performance is optimized, i.e. an optimal controller should be designed by minimizing the cost function.

To address these challenges, we formulate the problem within the framework of the linear optimal output regulation problem (LOORP), focusing on designing a feedback controller to achieve the asymptotic tracking with disturbance rejection. In the LOORP framework, the bupivacaine input is regarded as a bounded external signal d_k satisfying $\sup_{k\in\mathbb{Z}_+} \|d_k\| \leq \bar{d}$, system (5) can be rewritten as follows:

$$\begin{aligned} x_{k+1} &= Ax_k + Bu_k + Dd_k, \\ r_{k+1} &= Er_k, \\ e_k &= Cx_k + Fr_k, \end{aligned} \tag{7}$$

where $E = 1$, $F = -1$, $r_k \in \mathbb{R}$ is the reference value of MAP, $e_k \in \mathbb{R}$ is the tracking error. The linear output regulation problem (LORP) can be formulated as follows. For system (7) with $d_k \equiv 0$, the following feedback controller is designed

$$u_k = -Kx_k + Lr_k \tag{8}$$

such that the closed-loop system is asymptotically stable, i.e. $(A - BK)$ is Schur, and the tracking error e asymptotically converges to 0, where $K \in \mathbb{R}^{1\times 5}$ is feedback control gain and $L \in \mathbb{R}$ is feedforward control gain. In cases where the controller is required to be optimal based on a predefined cost, the problem is known as LOORP.

In this paper, it can be verified that the system (A, B) is controllable, and for all $\lambda \in \sigma(E)$, the matrix

$$\begin{bmatrix} A - \lambda I & B \\ E & 0 \end{bmatrix}$$

is of full rank. By selecting an admissible K such that the closed-loop system satisfies $(A - BK)$ is Schur, the LORP is considered solvable by the controller (8) if there exist matrices $X \in \mathbb{R}^{5\times 1}$ and $U \in \mathbb{R}$ that satisfy the following regulator equations [29],

$$\begin{aligned} XE &= AX + BU, \\ 0 &= CX + F, \end{aligned} \tag{9}$$

with

$$L = U + KX. \tag{10}$$

Without loss of generality, the LOORP can be solved in two subproblems.

Problem 1.

$$\begin{aligned} &\min_{X,U} \quad \mathrm{Tr}\left(X^{\mathrm{T}}\bar{Q}X + U^{\mathrm{T}}\bar{R}U\right) \\ &\text{subject to (9)}, \end{aligned} \tag{11}$$

where $\bar{Q} = \bar{Q}^{\mathrm{T}} \succ 0$, $\bar{R} = \bar{R}^{\mathrm{T}} \succ 0$.

Letting $\bar{x}_k = x_k - X^* r_k$, $\bar{u}_k = u_k - U^* r_k$, directly, the error system is as follows:

$$\begin{aligned} \bar{x}_{k+1} &= A\bar{x}_k + B\bar{u}_k, \\ e_k &= C\bar{x}_k. \end{aligned} \tag{12}$$

Problem 2.

$$\begin{aligned} &\min_{\bar{u}} \sum_{j=0}^{\infty} (\bar{x}_j^{\mathrm{T}} Q \bar{x}_j + \bar{u}_j^{\mathrm{T}} R \bar{u}_j) \\ &\text{subject to (12)}, \end{aligned} \tag{13}$$

where $Q = Q^{\mathrm{T}} \succ 0$, $R = R^{\mathrm{T}} \succ 0$.

Problem 2 is in the context of linear quadratic regulator (LQR) problem. According to the theory of linear optimal control [30], there exists a unique solution $P^* = P^{*\mathrm{T}} \succ 0$ to the following algebraic Riccati equation (ARE):

$$\begin{aligned} &A^{\mathrm{T}}PA - P + Q \\ &\quad - A^{\mathrm{T}}PB(R + B^{\mathrm{T}}PB)^{-1}B^{\mathrm{T}}PA = 0. \end{aligned} \tag{14}$$

The optimal feedback gain K^* can be obtained as

$$K^* = (R + B^{\mathrm{T}}P^*B)^{-1}B^{\mathrm{T}}P^*A. \tag{15}$$

The solution to the LOORP can be divided into two parts. Firstly, addressing the Problem 1 by solving the regulator Eq. (9) to obtain the optimal steady-state solution (X^*, U^*) while simultaneously deriving the feedforward control gain $L^* = U^* + K^*X^*$. Next, addressing the Problem 2 by computing the optimal feedback control gain K^*. Then, the LOORP solution is achieved, i.e. the optimal controller is given by

$$u_k^* = -K^*x_k + L^*r_k. \tag{16}$$

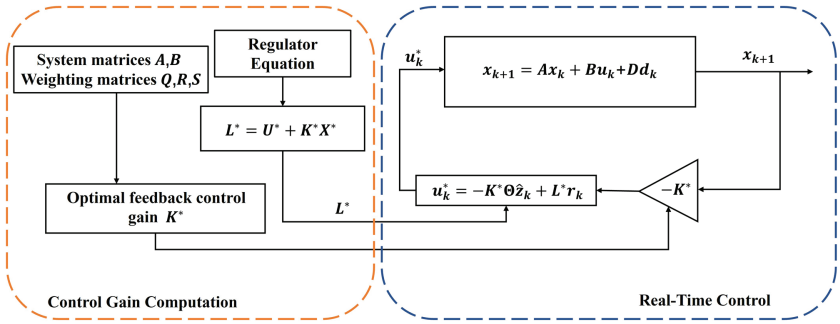

Fig. 1. Block diagram of the control structure.

Remark 1. The weights $(\bar{Q}, \bar{R})$ in Problem 1 are used to determine the optimal solution (X^*, U^*). These weights only affect the optimal feedforward gain $L^* = U^* + K^*X^*$, which determines the baseline PE infusion required to maintain MAP near the target. The weights (Q, R) in Problem 2 are used to compute the optimal feedback control gain K^* via the algebraic Riccati equation, ensuring closed-loop stability and satisfactory transient performance. Furthermore, it is worth noting that the optimal feedback control gain K^* does not rely on X^*, U^*. Therefore, Problems 1 and 2 can be solved independently.

3.3. *Optimal output-feedback controller*

In Sec. 3.2, we propose an optimal state-feedback controller design scheme by solving the LOORP. However, such controllers require full-state measurement to implement state-feedback control. The requirement usually cannot be satisfied in the blood pressure regulation during anesthesia. Specifically, some system states lack physiological interpretability and cannot be measured in clinical settings. This measurement limitation makes direct implementation of an optimal state-feedback feedforward controller infeasible for blood pressure control.

To overcome this challenge, we integrate the state reconstruction technique from Sec. 3.1 with our optimal controller design from Sec. 3.2. Following Lemma 3.1 which establishes the state reconstruction relationship $x_k = \Theta z_k$ through measurable outputs and substituting (6) into (16), an optimal output-feedback controller can be expressed as $u_k^* = -K^*\Theta z_k + L^*r_k$. Considering the fact that the bupivacaine input d_k is not measurable for feedback, the following output-feedback controller is finally developed

$$u_k^* = -K^*\Theta\hat{z}_k + L^*r_k, \tag{17}$$

where

$$\hat{z}_k = [u_{k-1}, 0, u_{k-2}, 0, u_{k-3}, 0, u_{k-4}, 0, u_{k-5}, 0, \bar{y}_{k-1,\,k-5}^{\mathrm{T}}]^{\mathrm{T}}.$$

By leveraging state reconstruction techniques, the implementation of the output-feedback controller (17) needs only measurable MAP data and drug delivery records to achieve control of the blood pressure. The block digram of the control structure is depicted in the Fig. 1.

4. Stability Analysis

In this section, we will analyze the stability of the closed-loop system with the developed output-feedback controller and unmeasurable but bounded bupivacaine input d_k.

Theorem 4.1. *The system* (7) *in closed-loop with the control policy* (17) *is practically stable.*

Proof. The closed-loop system (7) with (17) can be rewritten by

$$\begin{aligned}
\bar{x}_{k+1} &= Ax_k + Bu_k^* + Dd_k - X^*r_{k+1} \\
&= Ax_k - BK^*\Theta\hat{z}_k + Dd_k + BL^*r_k - X^*Er_k \\
&= Ax_k - BK^*\Theta(z_k - \tilde{z}_k) + Dd_k + BU^*r_k \\
&\quad + BK^*X^*r_k - AX^*r_k - BU^*r_k \\
&= A\bar{x}_k - BK^*(\Theta z_k - X^*r_k) + BK^*\Theta\tilde{z}_k + Dd_k \\
&= (A - BK^*)\bar{x}_k + BK^*\Theta\tilde{z}_k + Dd_k \\
&= (A - BK^*)\bar{x}_k + \Delta_k,
\end{aligned} \tag{18}$$

where $\Delta_k = BK^*\Theta\tilde{z}_k + Dd_k$ and

$$\begin{aligned}
\tilde{z}_k &= z_k - \hat{z}_k \\
&= [0, d_{k-1}, 0, d_{k-2}, 0, d_{k-3}, 0, d_{k-4}, 0, d_{k-5}, 0, 0, 0, 0, 0]^{\mathrm{T}}.
\end{aligned}$$

As the bupivacaine input is bounded by $\sup_{k\in\mathbb{Z}_+}\|d_k\| \le \bar{d}$, it is checkable that $\sup_{k\in\mathbb{Z}_+}\|\Delta_k\| \le (\sqrt{5}\|BK^*\Theta\| + \|D\|)\bar{d} := \bar{\Delta}$. Moreover, the ARE (14) implies that

$$(A - BK^*)^{\mathrm{T}}P^*(A - BK^*) - P^* + Q + (K^*)^{\mathrm{T}}RK^* = 0. \tag{19}$$

By choosing a Lyapunov function $V_k = \bar{x}_k^{\mathrm{T}}P^*\bar{x}_k$, the difference of the Lyapunov function along the trajectory of the

system (18) satisfies

$$
\begin{aligned}
V_{k+1} - V_k &= \bar{x}_{k+1}^{\mathrm{T}} P^* \bar{x}_{k+1} - \bar{x}_k^{\mathrm{T}} P^* \bar{x}_k \\
&= ((A - BK^*)\bar{x}_k + \Delta_k)^{\mathrm{T}} P^* ((A - BK^*)\bar{x}_k + \Delta_k) \\
&\quad - \bar{x}_k^{\mathrm{T}} P^* \bar{x}_k \\
&= \bar{x}_k^{\mathrm{T}} [(A - BK^*)^{\mathrm{T}} P^* (A - BK^*) - P^*] \bar{x}_k \\
&\quad + 2\bar{x}_k^{\mathrm{T}} P^* \Delta_k + \Delta_k^{\mathrm{T}} P^* \Delta_k \\
&= -\bar{x}_k^{\mathrm{T}} [Q + (K^*)^{\mathrm{T}} R K^*] \bar{x}_k + 2\bar{x}_k^{\mathrm{T}} P^* \Delta_k + \Delta_k^{\mathrm{T}} P^* \Delta_k \\
&\le -\bar{x}_k^{\mathrm{T}} [Q + (K^*)^{\mathrm{T}} R K^*] \bar{x}_k + \frac{\lambda_m(Q)}{2} \|\bar{x}_k\|^2 \\
&\quad + \frac{2}{\lambda_m(Q)} \|P^*\|^2 \|\Delta_k\|^2 + \|P^*\| \|\Delta_k\|^2 \\
&\le -\bar{x}_k^{\mathrm{T}} \left[Q - \frac{\lambda_m(Q)}{2} I + (K^*)^{\mathrm{T}} R K^* \right] \bar{x}_k \\
&\quad + \left(\frac{2}{\lambda_m(Q)} \|P^*\|^2 + \|P^*\| \right) \|\Delta_k\|^2 \\
&\le -\bar{x}_k^{\mathrm{T}} \left[Q - \frac{\lambda_m(Q)}{2} I + (K^*)^{\mathrm{T}} R K^* \right] \bar{x}_k \\
&\quad + \left(\frac{2}{\lambda_m(Q)} \|P^*\|^2 + \|P^*\| \right) \bar{\Delta}^2, \qquad (20)
\end{aligned}
$$

which immediately implies the practical stability of the closed-loop system (18). The proof is thus completed. □

5. Simulation Results

In this section, we evaluate the performance of the controller designed from the ARX-based state-space representation by implementing it in a simulated surgery.

In this simulation, the MAP is initially set to 80 mmHg with a total simulation duration of 90 min. Once the surgery was underway for five minutes, bupivacaine is infused to simulate obstetric anesthesia, which causes a decrease in MAP. Throughout the entire simulation, stochastic disturbances are introduced to the MAP signal to simulate fluctuations caused by physiological changes in the human body. Under the designed controller, the MAP is expected to stay around 85 mmHg.

To emulate physiological fluctuations and sensor noise during obstetric anesthesia, an additive stochastic disturbance was injected into the MAP-related state in the simulation. The disturbance d_k is selected as a zero-mean uniform white noise.

As shown in Fig. 2, the simulation results show that the optimal controller effectively regulates MAP fluctuations around the setpoint with minimal overshoot and a short response time. These results confirm the robustness of the

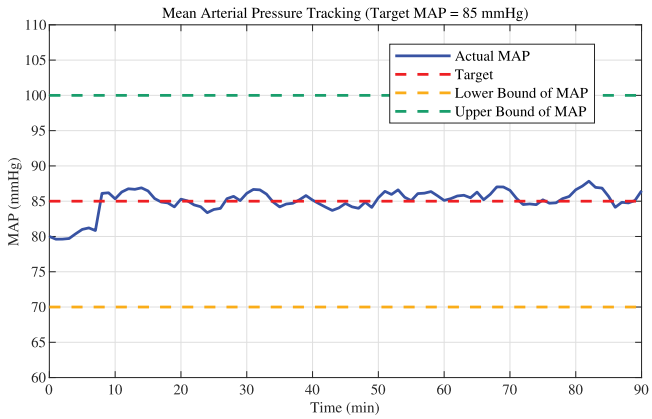

Fig. 2. The simulation results of MAP regulation using the optimal output-feedback controller.

controller and its effective tracking performance under disturbances. The controller exhibits a fast response and robust disturbance rejection, ensuring clinically reliable blood pressure regulation during obstetric anesthesia.

In our MAP regulation framework, an optimal output-feedback controller relies on state reconstruction techniques that reconstructs the full system states from the available input and output data. As shown in Fig. 3, the reconstructed states closely follow the actual system dynamics, enabling the controller to maintain the MAP at the 85 mmHg setpoint even in the presence of disturbances such as bupivacaine infusion or blood pressure fluctuations occurs. The minimal difference between estimated and actual MAP values demonstrates the high accuracy and reliability of the state reconstruction technique, which is essential for designing an effective output-feedback controller.

The PE infusion rate generated by the optimal output-feedback controller is shown in Fig. 4. When bupivacaine is administered at 5 min, the controller rapidly increases the PE infusion.

Figure 5 shows modifying the weighting matrix Q changes the aggressiveness of the blood pressure control system. Smaller Q values reduce overshoot but increase the settling time, whereas larger Q values enhance the responsiveness at the cost of larger overshoot. This trade-off is particularly clear when a disturbance is introduced between 5 min and 10 min.

Figure 6 shows the system response to varying bupivacaine infusion rates administered during the 5–10 min of the simulated surgery, representing different levels of MAP reductions during anesthesia. In all cases, the controller regulates MAP quickly to a small range around the setpoint despite large variations in drug dosage, demonstrating robustness to patient-specific reactions and maintaining hemodynamic stability throughout surgery.

As shown in Fig. 7, the control system shows consistent performance across different initial MAP values (80,

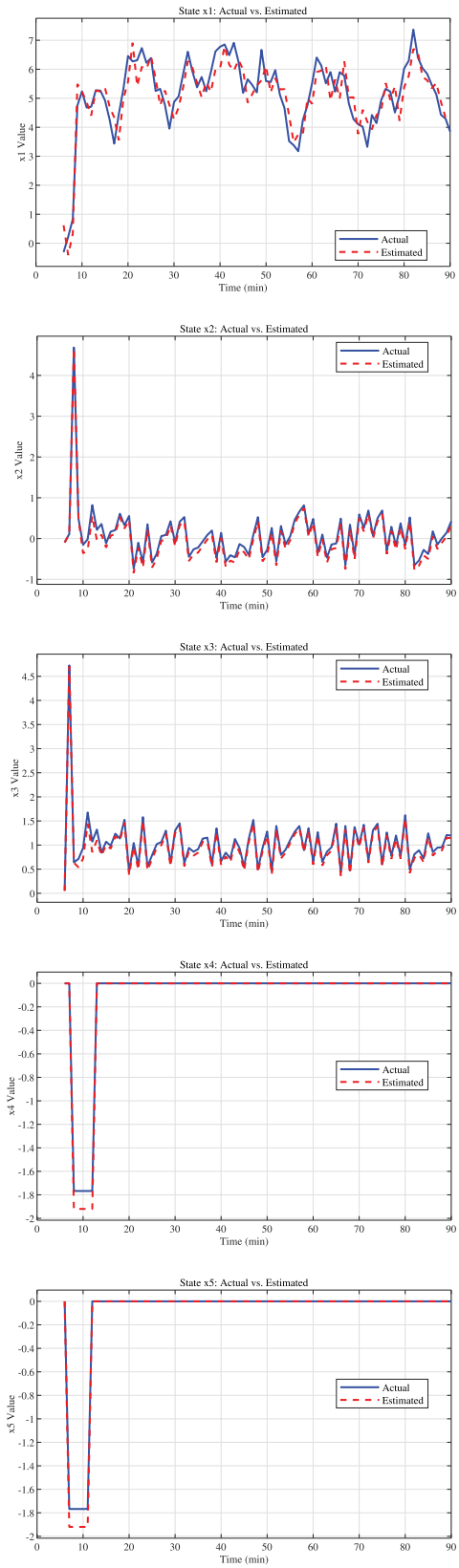

Fig. 3. Comparison of the reconstructed state values and the actual state values under disturbance.

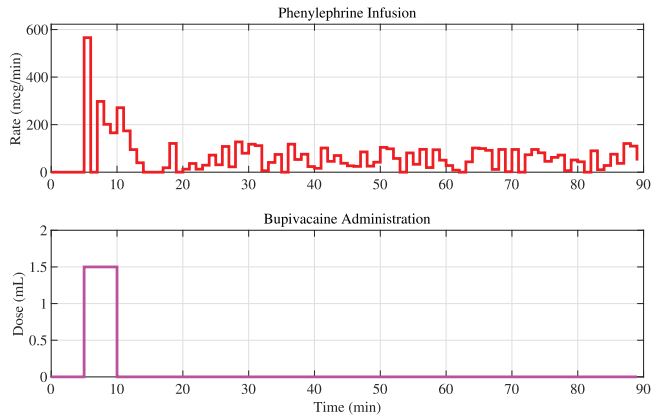

Fig. 4. The phenylephrine infusion rate generated by the optimal output-feedback controller.

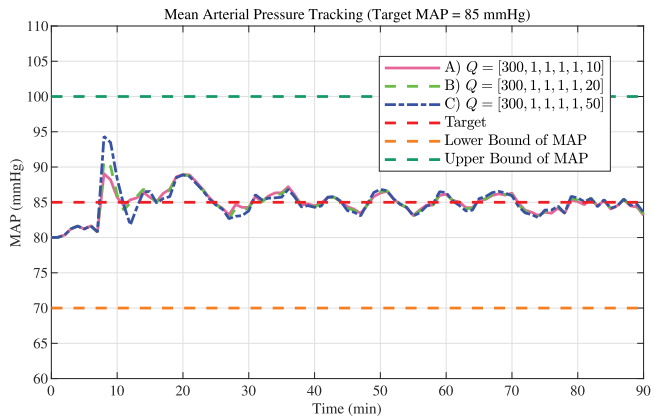

Fig. 5. The MAP trajectory with different Q matrices, with the initial value set to 80 mmHg and the setpoint at 85 mmHg.

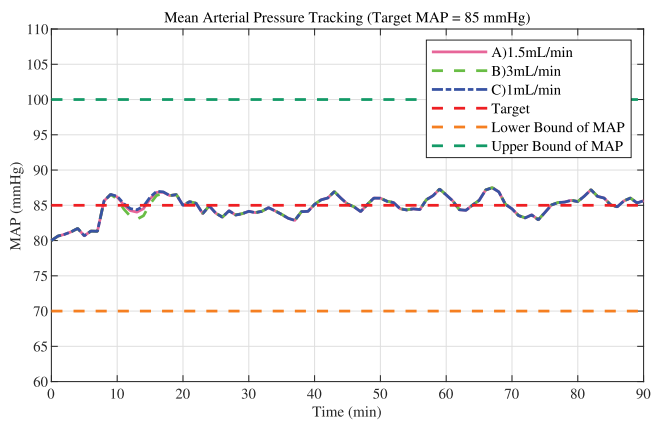

Fig. 6. Closed-loop control maintains MAP during variable bupivacaine infusion rates in simulated obstetric anesthesia.

85, and 90 mmHg) when regulating to the target set point of 85 mmHg. The results indicate that the proposed control method maintains robustness regardless of initial condition of MAP.

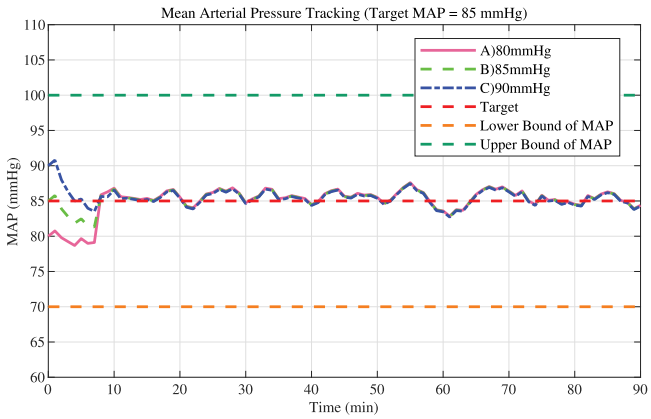

Fig. 7. Closed-loop control performance under varied initial MAPs (80, 85, 90 mmHg).

6. Discussion

Our optimal output-feedback controller is designed based on a state-space representation that is directly derived from an ARX model. This approach preserves the simplicity of the ARX model while achieving computational efficiency and explicit incorporation of physiological time delays, such as PE uptake and placental transfer dynamics. The linear ARX structure simplifies parameter identification and avoids the computational burden of nonlinear models. This makes the controller well designed for medical devices with limited computing resources requiring real-time updates. Although nonlinear models may better capture high-dose saturation effects, their convergence challenges and high computational costs compromise clinical practicality where speed and reliability are critical. Despite the embedded physiological delays, the proposed controller (17) effectively compensates for transient hypotension. Simulation results show rapid disturbance rejection, minimal setpoint deviation, and stable blood pressure maintenance within safe ranges.

The linear and time invariant assumptions inherent in the ARX model limit its ability to represent the nonlinear, adaptive characteristics of maternal-fetal physiology, such as dynamic variations in placental resistance during uterine contractions and autonomic compensatory responses. Sensor artifacts and inter-patient variability under clinical conditions may challenge controller performance, highlighting the need for future model adaptation and experimental validation in noisy real-world conditions to ensure robustness and reliability.

A key factor in making the controller useful for clinical settings is carefully adjusting the weighting matrix Q, which controls the balance between response speed and overshoot. In obstetrics, this balance is critical for the safety of both the mother and the baby. For example, excessive PE administration may induce placental vasoconstriction, which can harm the fetus, especially in high-risk pregnancies with existing placenta problems. More conservative settings for Q prioritize stability, reducing overshoot but making the system slower to adjust. This may pose risks in cases of heavy bleeding or sudden low blood pressure, where delays could increase risks to the fetus. Conversely, more aggressive settings speed up the regulation of dangerous drops in blood pressure but can lead to transient oscillations. Therefore, safety mechanisms, such as dose limits and additional real-time monitoring should be taken into consideration to prevent over-infusion.

The simulation of different disturbances highlights how well the controller can adapt to various clinical situations. Gradual changes in blood pressure represent slow hypotension in patients with delayed drug absorption, where small adjustments in PE are enough. In contrast, abrupt drops, such as in emergencies like placental abruption, require quick adjustments to prevent organ damage from poor blood flow. The controller performs well in both of these situations and can work without needing patient-specific data, which is important for personalized care. However, studies still need to address several key challenges, such as the nonlinear effects of high-dose drugs and changes in placental resistance during delivery. Future research will develop machine learning algorithms to establish high-fidelity nonlinear models capturing physiological complexities and incorporate adaptive control algorithms to enable real-time, patient-specific blood pressure regulation, ensuring computational efficiency and clinical interpretability while addressing inter-patient variability.

7. Conclusion

This paper presents an output-feedback control method for automated blood pressure regulation during obstetric anesthesia under sympathetic blockade. Starting from an existing ARX model, we convert it into a state-space representation to directly integrate with optimal control theory. We introduce a state reconstruction algorithm that exploits only the available input-output data to estimate unmeasured states, thereby enabling reliable output-feedback control despite limited real-time measurements. Simulation results demonstrate robust setpoint tracking and strong disturbance rejection, confirming the method's effectiveness for MAP regulation.

The proposed controller, which combines optimal feedback control with feedforward control, achieves rapid adjustments and robust performance when evaluated under simulated clinical conditions. Theoretical analysis further confirms that the closed-loop system remains stable despite model uncertainties, offering a solid safety foundation for potential clinical implementation.

Although the linear model works well for fast real-time computation, it has limitations in capturing more complex,

nonlinear body responses, such as variations in placental resistance. Therefore, further improvements are necessary. Future research will focus on incorporating adaptive parameter tuning and performing validation experiments.

Acknowledgments

The work has been supported in part by the National Key R&D Program of China under Grant No. 2024 YFA 101 2700, the National Natural Science Foundation of China (NSFC) under Grant Nos. 62373090 and 62521001, and the Liaoning Revitalization Talents Program under Grant No. XLYC2403177. The authors thank Dr. Sherwin Davoud for the fruitful discussions.

ORCID

Zijian Yang
https://orcid.org/0009-0005-2990-3670
Yuchen Dong
https://orcid.org/0009-0004-5272-4059
Weinan Gao
https://orcid.org/0000-0001-7921-018X
Quan Na
https://orcid.org/0009-0002-6643-6723
Tengfei Liu
https://orcid.org/0000-0002-3969-7605

References

[1] J. L. Hawkins, Epidural analgesia for labor and delivery, *New England J. Med.* **362**(16) (2010) 1503–1510.
[2] S. H. Halpern and V. Walsh, Epidural ropivacaine versus bupivacaine for labor: A meta-analysis, *Anesth. Analg.* **96**(5) (2003) 1473–1479.
[3] H. S. Downs and P. H. Morrison, The effects of spinal anesthesia on the fetal heart rate, *California Med.* **99**(6) (1963) 374.
[4] T. Thoren, B. Holmström, N. Rawal, J. Schollin, S. Lindeberg and G. Skeppner, Sequential combined spinal epidural block versus spinal block for cesarean section: Effects on maternal hypotension and neurobehavioral function of the newborn, *Anesth. Analg.* **78**(6) (1994) 1087–1092.
[5] J. Fitzgerald, K. Fedoruk, S. Jadin, B. Carvalho and S. Halpern, Prevention of hypotension after spinal anaesthesia for caesarean section: A systematic review and network meta-analysis of randomised controlled trials, *Anaesthesia* **75**(1) (2020) 109–121.
[6] H. S. Tan, S. Nagarajan, J. J. I. Chan, C. W. Tan, R. Sultana, A. T. H. Sia and B. L. Sng, Evaluating an advanced double intravenous vasopressor automated system to treat hypotension during spinal anesthesia for cesarean delivery: A randomized controlled trial, *BMC Anesthesiol.* **23**(1) (2023) 33.
[7] J. Mitra, J. Roy, P. Bhattacharyya, M. Yunus and N. Lyngdoh, Changing trends in the management of hypotension following spinal anesthesia in cesarean section, *J. Postgrad. Med.* **59**(2) (2013) 121–126.
[8] S. Ahmed, E. Ahmad, E. Fatima, U. Akram, O. Ur Rehman, A. Harikrishna, S. Sharif, N. Akmal and A. J. Nashwan, Efficacy and safety of norepinephrine versus phenylephrine for post-spinal hypotension in preeclamptic patients: A systematic review and meta-analysis, *Euro. J. Obstetr. Gynecol. Reproduct. Biol.* **303** (2024) 91–98.
[9] W. N. Kee, A random-allocation graded dose-response study of norepinephrine and phenylephrine for treating hypotension during spinal anesthesia for cesarean delivery, *Obstetric Anesth. Digest* **38**(3) (2018) 161–162.
[10] R. Diversi, R. Guidorzi and U. Soverini, Identification of arx models with noisy input and output, *2007 European Control Conf. (ECC)* (IEEE, 2007), pp. 4073–4078.
[11] S. Dusitkasem, B. H. Herndon, M. Somjit, D. L. Stahl, E. Bitticker and J. C. Coffman, Comparison of phenylephrine and ephedrine in treatment of spinal-induced hypotension in high-risk pregnancies: A narrative review, *Front. Med.* **4** (2017) 2.
[12] W. Wang, T. Chai, H. Wang and Z. Wu, Signal-compensation-based adaptive PID control for fused magnesia smelting processes, *IEEE Trans. Indust. Electron.* **70**(9) (2022) 9441–9451.
[13] T. Chai, Z. Zhou, S. Cheng, Y. Jia and Y. Song, Industrial metaverse-based intelligent PID optimal tuning system for complex industrial processes, *IEEE Trans. Cybernet.* **54**(11) (2024) 6458–6470.
[14] Y. Dong and W. Gao, Cooperative adaptive optimal output regulation of multi-agent systems with an application to connected and autonomous vehicles, *2024 IEEE 7th Int. Conf. Industrial Cyber-Physical Systems (ICPS)* (IEEE, 2024), pp. 1–6.
[15] W. Gao, T. Chai, N. Qiao and Y. Liu, String stable platooning control based on adaptive dynamic programming, *2024 8th CAA Int. Conf. Vehicular Control and Intelligence (CVCI)* (IEEE, 2024), pp. 1–6.
[16] F. W. Chapman, J. C. Newell and R. J. Roy, A feedback controller for ventilatory therapy, *Ann. Biomed. Eng.* **13** (2006) 359–372.
[17] M. Di Ferdinando, P. Pepe, P. Palumbo, S. Panunzi and A. De Gaetano, Semiglobal sampled-data dynamic output feedback controller for the glucose-insulin system, *IEEE Trans. Control Syst. Technol.* **28**(1) (2020) 16–32.
[18] A. Sharma, H. P. Singh and Nilam, A methodical survey of mathematical model-based control techniques based on open and closed loop control approach for diabetes management, *Int. J. Biomath.* **15**(7) (2022) 2250051.
[19] A. Khani, P. Bagheri, M. Baradarannia and A. Mohammadzadeh, Artificial intelligent pancreas for type 1 diabetic patients using adaptive type 3 fuzzy fault tolerant predictive control, *Eng. Appl. Artif. Intell.* **139** (2025) 109627.
[20] K. Sagawa, Closed-loop physiological control of the heart, *Ann. Biomed. Eng.* **8** (1980) 415–429.
[21] T. Kitamura, K. Matsuda and H. Akashi, Adaptive control technique for artificial hearts, *IEEE Trans. Biomed. Eng.* **BME-33**(9) (1986) 839–844.
[22] N. Malagutti, A. Dehghani and R. A. Kennedy, Robust control design for automatic regulation of blood pressure, *IET Control Theory Appl.* **7**(3) (2013) 387–396.
[23] S. Davoud, W. Gao and E. Riveros-Perez, Adaptive optimal target controlled infusion algorithm to prevent hypotension associated with labor epidural: An adaptive dynamic programming approach, *ISA Trans.* **100** (2020) 74–81.
[24] F. L. Lewis and K. G. Vamvoudakis, Reinforcement learning for partially observable dynamic processes: Adaptive dynamic programming using measured output data, *IEEE Trans. Syst. Man Cybernet. Part B (Cybernetics)* **41**(1) (2011) 14–25.
[25] W. Gao, Y. Jiang, Z. P. Jiang and T. Chai, Adaptive and optimal output feedback control of linear systems: An adaptive dynamic programming approach, in *Proc. 11th World Congress on Intelligent Control and Automation* (IEEE, 2014), pp. 2085–2090.
[26] S. C. Davoud, B. Ozaslan, E. M. Aiello, R. Kleinlein, B. Eberhard, H. Hassan, F. J. Doyle III and V. P. Kovacheva, Empirical pharmacodynamic model of phenylephrine and intrathecal bupivacaine for mean

arterial pressure prediction in obstetric patients presenting for elective cesarean delivery under spinal anesthesia, *J. Clinic. Monitor. Comput.* **39**(4) (2025) 775–785.
[27] Y. Liu, A. Birch and R. Allen, Dynamic cerebral autoregulation assessment using an ARX model: Comparative study using step response and phase shift analysis, *Med. Eng. Phys.* **25**(8) (2003) 647–653.
[28] W. Aangenent, D. Kostic, B. de Jager, R. van de Molengraft and M. Steinbuch, Data-based optimal control, in *Proceedings of the 2005, American Control Conference*, Vol. 2 (IEEE, Portland, OR, USA, 2005), pp. 1460–1465.
[29] W. Gao and Z. P. Jiang, Adaptive dynamic programming and adaptive optimal output regulation of linear systems, *IEEE Trans. Autom. Control* **61**(12) (2016) 4164–4169.
[30] F. L. Lewis, D. Vrabie and V. L. Syrmos, *Optimal Control* (John Wiley & Sons, 2012).

Zijian Yang received the B.S. degree in Materials Science and Engineering from Northeastern University, Shenyang, P. R. China, in 2024, and also the B.S. degree in Electrical Power and Automation Engineering from Université Toulouse III — Paul Sabatier, Toulouse, France, in 2024. He is currently pursuing the M.S. degree at the State Key Laboratory of Synthetical Automation for Process Industries, Northeastern University. His research interests include linear quadratic control, optimal control, and data-driven control.

Yuchen Dong received the B.S. degree in the School of Mathematical Sciences from Heilongjiang University in 2019 and the M.S. degree in the School of Artificial Intelligence from Hebei University of Technology in 2023. She is currently pursuing her Ph.D. at the State Key Laboratory of Synthetical Automation for Process Industries, Northeastern University. Her research interest includes network attacks, reinforcement learning, data-driven, and resilient control.

Weinan Gao, received the B.Sc. degree in automation and the M.Sc. degree in control theory and control engineering from Northeastern University, Shenyang, P. R. China, in 2011 and 2013, respectively, and the Ph.D. degree in electrical engineering from New York University, Brooklyn, NY, USA, in 2017. He was an Assistant Professor in mechanical and civil engineering with the Florida Institute of Technology, Melbourne, FL, USA; an Assistant Professor in electrical and computer engineering with Georgia Southern University, Statesboro, GA, USA; and a Visiting Professor with the Mitsubishi Electric Research Laboratory, Cambridge, MA, USA. He is currently a Professor with the State Key Laboratory of Synthetical Automation for Process Industries, Northeastern University. His research interests include reinforcement learning, adaptive dynamic programming, optimal control, cooperative adaptive cruise control, intelligent transportation systems, sampled-data control systems, and output regulation theory. Dr. Gao is the recipient of the Best Paper Award at IEEE Data Driven Control and Learning Systems Conference in 2023 and IEEE International Conference on Real-Time Computing and Robotics in 2018 and the David Goodman Research Award at New York University in 2019. He is an Associate Editor for IEEE TRANSACTIONS ON NEURAL NETWORKS AND LEARNING SYSTEMS, IEEE/CAA JOURNAL OF AUTOMATICA SINICA and Control Engineering Practice. He is a Member of the Technical Committee (TC) on Nonlinear Systems and Control of the IEEE Control Systems Society and the TC 1.2 Adaptive and Learning Systems of the International Federation of Automatic Control.

Quan Na received the Ph.D. degree in obstetrics and gynecology from China Medical University, Shenyang, P. R. China, and completed a postdoctoral fellowship in obstetrics and maternal-fetal medicine at Johns Hopkins University, Baltimore, MD, USA. She is the Principal Investigator of projects funded by the National Natural Science Foundation of China and has served as a key member of the National Key Research and Development Program, as well as the Principal Investigator of the Liaoning Provincial Science and Technology Program.

Dr. Na is the recipient of the Second Prize and Third Prize of the Liaoning Provincial Science and Technology Progress Awards.

She previously served as the Secretary of the Liaoning Provincial Obstetrics and Gynecology Society of the Chinese Medical Association and as a committee member of the Pregnancy Immunology Branch of the Liaoning Society of Immunology, among other professional appointments.

Her research interests include the prevention and treatment of preterm birth, as well as the mechanisms underlying neurodevelopmental injury and developmental disorders in preterm infants.

Tengfei Liu, received the B.E. degree in automation and the M.E. degree in control theory and control engineering from South China University of Technology, Guangzhou, P. R. China, in 2005 and 2007, respectively, and the Ph.D. degree in engineering from RSISE, Australian National University, Canberra, ACT, Australia, in 2011. From 2011 to 2013, he was a Postdoctoral Researcher with the Faculty Fellowship, Polytechnic Institute of New York University, Brooklyn, NY, USA. Since 2014, he has been a Faculty Member with the State Key Laboratory of Synthetical Automation for Process Industries, Northeastern University, Shenyang, P. R. China. His research interests include stability and control of interconnected nonlinear systems.